

Isoprene fluxes measured by enclosure, relaxed eddy accumulation, surface layer gradient, mixed layer gradient, and mixed layer mass balance techniques

Alex Guenther, William Baugh, Ken Davis, Gary Hampton,¹
Peter Harley, Lee Klinger, Lee Vierling, and Patrick Zimmerman
Atmospheric Chemistry Division, National Center for Atmospheric Research, Boulder, Colorado

Eugene Allwine, Steve Dilts, Brian Lamb, and Hal Westberg
Department of Civil and Environmental Engineering, Washington State University, Pullman

Dennis Baldocchi
Atmospheric Turbulence and Diffusion Division, NOAA, Oak Ridge, Tennessee

Chris Geron and Thomas Pierce
U.S. Environmental Protection Agency, Research Triangle Park, North Carolina

Abstract. Isoprene fluxes were estimated using eight different measurement techniques at a forested site near Oak Ridge, Tennessee, during July and August 1992. Fluxes from individual leaves and entire branches were estimated with four enclosure systems, including one system that controls leaf temperature and light. Variations in isoprene emission with changes in light, temperature, and canopy depth were investigated with leaf enclosure measurements. Representative emission rates for the dominant vegetation in the region were determined with branch enclosure measurements. Species from six tree genera had negligible isoprene emissions, while significant emissions were observed for *Quercus*, *Liquidambar*, and *Nyssa* species. Above-canopy isoprene fluxes were estimated with surface layer gradients and relaxed eddy accumulation measurements from a 44-m tower. Midday net emission fluxes from the canopy were typically 3 to 5 mg C m⁻² h⁻¹, although net isoprene deposition fluxes of -0.2 to -2 mg C m⁻² h⁻¹ were occasionally observed in early morning and late afternoon. Above-canopy CO₂ fluxes estimated by eddy correlation using either an open path sensor or a closed path sensor agreed within ±5%. Relaxed eddy accumulation estimates of CO₂ fluxes were within 15% of the eddy correlation estimates. Daytime isoprene mixing ratios in the mixed layer were investigated with a tethered balloon sampling system and ranged from 0.2 to 5 ppbv, averaging 0.8 ppbv. The isoprene mixing ratios in the mixed layer above the forested landscape were used to estimate isoprene fluxes of 2 to 8 mg C m⁻² h⁻¹ with mixed layer gradient and mixed layer mass balance techniques. Total foliar density and dominant tree species composition for an approximately 8100 km² region were estimated using high-resolution (30 m) satellite data with classifications supervised by ground measurements. A biogenic isoprene emission model used to compare flux measurements, ranging from leaf scale (10 cm²) to landscape scale (10² km²), indicated agreement to within ±25%, the uncertainty associated with these measurement techniques. Existing biogenic emission models use isoprene emission rate capacities that range from 14.7 to 70 μg C g⁻¹ h⁻¹ (leaf temperature of 30°C and photosynthetically active radiation of 1000 μmol m⁻² s⁻¹) for oak foliage. An isoprene emission rate capacity of 100 μg C g⁻¹ h⁻¹ for oaks in this region is more realistic and is recommended, based on these measurements.

1. Introduction

Elevated surface ozone concentrations are a persistent pollution problem in many industrialized countries. Ozone

control is difficult because tropospheric ozone production is the result of a complex set of photochemical reactions and precursor emissions, with significant contributions from natural sources. Natural emissions of volatile organic compounds (VOC) exceed anthropogenic emissions on a global scale. Recognition of the important role of natural VOC has led to the incorporation of natural VOC emissions into the oxidant control strategies developed to combat high-ozone levels. The Biogenic Emissions Inventory System (BEIS) developed by Pierce and Waldruff [1991] has been widely used to

¹Now at Hampton Associates, Boulder, Colorado.

incorporate natural VOC emission estimates into ozone control strategies in both the United States and Europe. A more recent version of this model (BEIS2) includes improved methods for estimating landscape data and canopy environment [Geron *et al.*, 1994]. BEIS2 also utilizes updated emission rate capacities [Guenther *et al.*, 1994], and experimentally verified relationships between emissions and environmental conditions [Guenther *et al.*, 1993]. The VOC emission rates estimated by BEIS2 for most landscapes range from slightly less than BEIS to as much as a factor of 5 higher [Geron *et al.*, 1995].

Geron *et al.* [1994] used the BEIS2 model to estimate natural VOC emissions from the eastern United States and found that isoprene from oak (*Quercus*) trees dominates daytime fluxes. A comprehensive field study of isoprene fluxes from a forested region with a significant oak component was conducted to evaluate the BEIS and BEIS2 models and the uncertainties associated with each model component. Representative isoprene emission characteristics for individual tree species were determined, based on isoprene flux measurements from individual leaves and branches. Isoprene fluxes in the surface layer above the forest canopy were used to investigate net (emission minus deposition) canopy fluxes and to evaluate emission models for a region where land cover and environmental conditions were characterized in detail. The ability of emission models to estimate fluxes on the scales used in regional photochemical models (10^2 km²) was tested with measurements that characterized the daytime mixed layer. Specific components of this study are described in detail elsewhere [Baldocchi *et al.*, 1995; P. Harley *et al.*, Environmental controls over isoprene emission from sun and shade leaves in a deciduous oak canopy, submitted to *Tree Physiology*, 1996b; Lamb *et al.*, 1996].

2. Methods

Field experiments were conducted in July and August 1992 within the Walker Branch Watershed located on a U.S. Department of Energy Reservation (35° 57' 30" N, 84° 17' 15" W, 365 m elevation) near Oak Ridge, Tennessee. Previous biogeochemical cycling studies at this site and general site characteristics are given by Johnson and van Hook [1989]. Fluxes were measured within three nested regions (Plate 1). The surface layer (SL) flux region has a radius of 0.5 km and is centered on a 44-m walkup tower that provided a platform for leaf and branch enclosures and for above-canopy flux measurement systems (relaxed eddy accumulation and surface layer gradients). The mixed layer gradient (MLG) and mixed layer mass balance (MB) regions are centered on a clearing, about 400 m north of the walkup tower, where a tethered balloon sampling system was deployed. The MLG region has a 3-km radius and includes the landscape that influences mixed layer gradient flux estimates. The MB region has a 14-km radius and includes the landscape influencing the mixed layer mass balance flux estimates. Previous studies have demonstrated that meaningful above-canopy surface layer flux estimates can be made with instruments on the 44-m tower even though it is located on a ridge in moderately complex terrain [Baldocchi and Harley, 1995; Verma *et al.*, 1986]. The meteorological conditions during the study were typical of summer in the eastern United States. Maximum photosynthetically active radiation (PAR) fluxes were over 1700 $\mu\text{mol m}^{-2} \text{s}^{-1}$. Above-

canopy winds ranged from about 0.1 to 4.6 m s⁻¹, predominately from the southwest (54%) and northeast (22%) quadrants that correspond to flow along the ridge. Temperatures during sampling periods ranged from 18° to 31°C (mean = 24.5°C), and relative humidity ranged from 40% to 87% (mean = 77%). The hot and humid afternoons were often accompanied by thunderstorms.

2.1. Land Cover Characterization

Thirty-one circular 30 m diameter (707 m²) plots were established along three transects located in representative vegetation types within the MLG and MB region. Each plot was sampled for species composition, diameter at breast height (dbh, ~1.5 m), tree height, seedling and sapling count, leaf area index, and percent cover of the dominant growth forms (evergreen scrub, deciduous shrub, ericaceous shrub, forb, graminoid, vine, lichen, pteridophyte, and moss). Individual trees were assigned to one of three classes: trees, > 10 cm dbh; saplings, dbh = 4 to 10 cm and height > 1.5 m; and seedlings, dbh < 4 cm or height < 1.5 m. In addition to the transects, an area of 3500 m² within the SL region was sampled for tree species composition and diameter at breast height information.

A land cover database for the Oak Ridge region was developed using a Landsat satellite Thematic Mapper (TM) classification image created from multitemporal imagery and supervised classification techniques, referred to here as the Thematic Mapper Land Cover (TMLC) database. The classification procedures and results will be described in detail elsewhere. The TMLC database has 30 m spatial resolution and covers an area of approximately 90 km X 90 km. The database contains 11 land cover classes: loblolly pine, mixed pine, regrowing (young) pine, high oak deciduous, medium oak deciduous, low oak deciduous, shrubs and grasses, agriculture, water, bare soil and urban. Four general categories are shown in Plate 1. Total foliar density and the fraction contributed by each tree species were estimated for each land cover class from forest statistics data collected in the 30-m circular plots.

2.2. Flux Measurement Techniques

Isoprene fluxes were estimated using the eight measurement systems listed in Table 1. The four systems used to estimate fluxes from individual leaves or branches included a portable leaf cuvette with environmental control (LEC), portable leaf cuvettes with no environmental control (LNC), a tower-mounted branch enclosure for investigating branches at different canopy depths (BCS) and a tripod-mounted branch enclosure for investigating lower branches of various tree species throughout the region (BRS). Two systems were used to estimate fluxes in the surface layer above the forest canopy: a relaxed eddy accumulation (REA) system and a system that estimated fluxes from isoprene gradient profiles and an eddy diffusivity based on eddy correlation measurements of water vapor (GPEC). Data collected with a tethered balloon system were used to estimate landscape scale fluxes using both a mixed layer gradient (MLG) technique and a mass balance (MB) technique.

Enclosure methods. Three of the enclosure systems (LEC, LNC, and BCS) are described in detail by P. Harley *et al.* (1996b). The LEC system consisted of an open path gas exchange system that provided control of temperature, light intensity, water vapor, and CO₂ concentration within the enclosure. The LNC system included three separate leaf

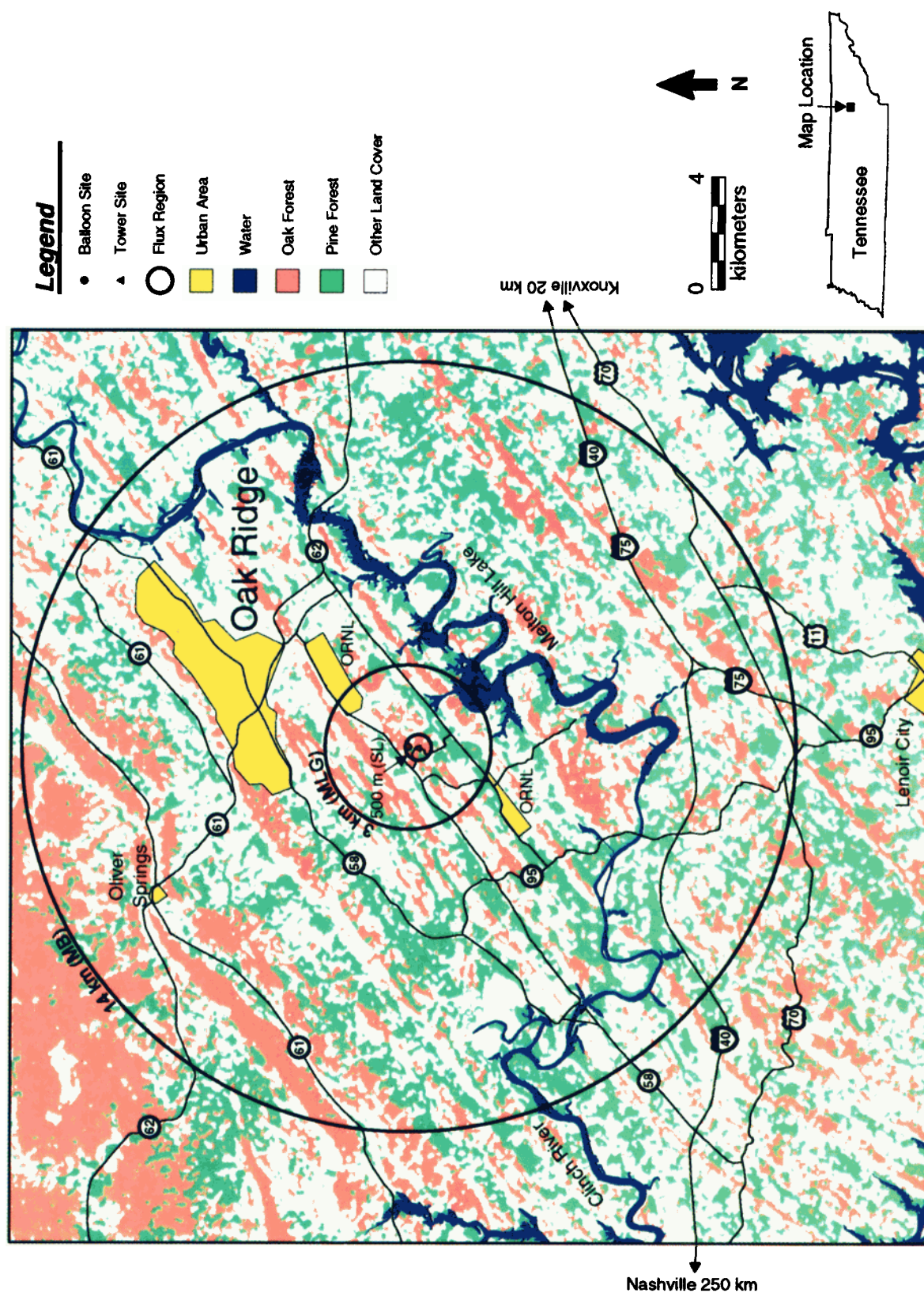


Plate 1. Land cover distribution and location of field sites.

Table 1. Description of Isoprene Flux Measurement Techniques

Flux Measurement Technique	Abbreviation	Sample Collection	Analytical Method
Enclosures (Leaf/Branch Scale: 0.001 to 1 m²)			
Leaf, with environmental control	LEC	glass syringe	GC-RGD
Leaf, without environmental control	LNC	glass syringe	GC-RGD
Branch, canopy survey	BCS	glass syringe	GC-RGD
Branch, regional survey	BRS	SS canisters	GC-FID
Surface layer (Canopy Scale: 0.001 to 1 km²)			
Relaxed eddy accumulation	REA	Teflon bags	GC-FID
Gradient profile, eddy correlation	GPEC	Teflon bags	GC-FID
Mixed layer (Landscape Scale: 10 to 1000 km²)			
Mixed-layer gradient	MLG	Teflon bags	GC-FID
Mass balance	MB	Teflon bags	GC-FID

Analytical methods include gas chromatography with reduction gas detector (GC-RGD) and gas chromatography with flame ionization detector (GC-FID)

cuvettes, while the BCS system consisted of a single branch enclosure. Samples of air exiting the enclosure were collected into glass syringes and analyzed with the gas chromatograph (GC) with reduction gas detector (RGD) described in section 2.3. Isoprene emission rates, E ($\mu\text{g C g}^{-1} \text{ h}^{-1}$), for individual leaves and branches were calculated as

$$E = f(C_o - C_i) b^{-1} \quad (1)$$

where f is the flow rate (cubic meters per hour) into the enclosure, C_o is the isoprene concentration (micrograms carbon per cubic meters) of the outlet airstream, C_i is the isoprene concentration (micrograms carbon per cubic meter) of the inlet airstream and b is the foliar mass (grams dry weight) within the enclosure.

The 30-L cylindrical enclosure used for the BRS system was constructed of Teflon film over a stainless steel support frame. The enclosure was supported by an external PVC pipe frame mounted on a camera tripod. Sweep air was supplied from compressed gas cylinders at flow rates of 10 to 12 L min⁻¹, measured with a mass flow meter. Ambient humidity and CO₂ levels were approximated in the sweep air by mixing hydrocarbon and CO₂ free air with hydrocarbon free air containing 2% CO₂ and then passing this air through distilled water. Ancillary measurements included leaf temperature, relative humidity, PAR, and CO₂ concentration. The entire apparatus was battery powered and mounted on a cart for mobility. Whole air samples from the enclosure were collected in Suma-deactivated stainless steel canisters and analyzed by GC with flame ionization detector (FID) described in section 2.3.

Surface layer methods. Isoprene fluxes in the surface layer above the forest canopy were measured by relaxed eddy accumulation and gradient profile methods. The data presented in this paper are the first measurements of isoprene fluxes with an REA system. Tracer and gradient profile methods have previously been used to measure isoprene fluxes [Lamb *et al.*, 1985; Lamb *et al.*, 1986]. Previous applications of the gradient profile method used indirect estimates of the relationship between scalar fluxes and gradients. Fluxes estimated by the REA and GPEC techniques are representative of the area within 500 m of the tower (shown as the SL region in Plate 1).

The 30-min average isoprene concentration gradients and eddy diffusivity estimates were used to estimate isoprene fluxes with the GPEC system. Whole air samples were collected from a 44-m walkup tower at heights of 28.8 m, 32.3 m, and 38 m above ground level (AGL). Concentration gradients were estimated by a least squares best fit. In some cases, concentrations were determined only at heights of 28.8 and 38 m. Samples were collected by pushing air with a Teflon diaphragm pump (KNF Neuberger, Princeton, N.J.) through 40-m Teflon lines and into evacuated 15-L Teflon bags located at the bottom of the tower. Samples were analyzed with the GC-FID system described in section 2.3. No significant difference in isoprene concentration was observed when air samples were pushed directly into Teflon bags placed on the tower at the 28.8-m and 38-m heights instead of sampling through the Teflon lines. The GPEC isoprene flux estimates assume similarity between water vapor fluxes and isoprene fluxes. A Lagrangian micrometeorological model was used to demonstrate that eddy diffusivities based on water vapor provide better results for isoprene flux estimates than eddy diffusivities based on CO₂, wind speed, or temperature [Baldocchi *et al.*, 1995]. We expected water vapor to be more representative of isoprene fluxes since both are unidirectional gas fluxes, while the CO₂ flux contains both a strong emission (from soils) and deposition (into the canopy) component. Eddy diffusivity estimates for water vapor, K (m² s⁻¹), were calculated from eddy covariance measurements of water vapor fluxes, $w'q'$, and the measured water vapor gradient, $\Delta q/\Delta z$, using the gradient flux relationship $K\Delta q/\Delta z = w'q'$.

Eddy covariance CO₂ and water fluxes were measured with two systems. One system used a three-dimensional sonic anemometer (Applied Technology SWS/3K, Boulder, Colorado) and a custom-made open path infrared gas analyzer (IRGA) [Baldocchi and Harley, 1995] and is referred to here as the EC-O system. The second system used a three-dimensional sonic anemometer (Applied Technology SWS/3K, Boulder, Colorado) with an analog signal digitizer and a closed path IRGA (LI-COR 6262, Lincoln, Nebraska) and is referred to here as the EC-C system. Isoprene fluxes, F , were then estimated from K and the measured isoprene gradient as $F = K \Delta C_i / \Delta z$.

The relaxed eddy accumulation system consisted of a three-dimensional sonic anemometer (Applied Technology, Inc., SWS/3K, Boulder, Colorado), a Teflon diaphragm pump (KNF Neuberger, Princeton, N.J.), three-port Teflon isolatch valves (General Valve Co., Fairfield, N.J.), a computer and control program, and a custom-designed pump control and valve control board. The pump control system provided a constant air flow through the REA system. Air was pulled into the pump through Teflon tubing (3 m length, 0.318 cm diameter) and immediately directed through valves into either a vent line, or one of two Teflon lines (40 m length, 0.635 cm diameter) leading to two 15-L evacuated Teflon bags located at the base of the tower. The three-port valves were switched at a maximum rate of 10 Hz to direct samples into the appropriate Teflon bag. The time required for input air to reach the three-port valves was matched to the processing time of the sonic anemometer, computer, and valve control board. After an approximately half-hour (1638.4 s) sampling period, air samples in the Teflon bags were analyzed with the GC-FID system described in section 2.3.

The REA system was deployed at a height of 30.5-m AGL on the walkup tower. Isoprene and CO₂ fluxes were estimated using the relationship described by *Businger and Oncley* [1990]

$$F = \beta (C_u - C_d) \sigma_w \quad (2)$$

where β is a nondimensional coefficient and C_u and C_d are the mean concentrations associated with updrafts and downdrafts, respectively. A 4-min running mean for vertical wind speed, w_o (meter per second), and standard deviation of vertical wind velocity, σ_w (meter per second), were calculated in real time and used to calculate the vertical wind speed threshold (w_T). This value was used to separate whole air samples into updraft ($w' > w_T$), downdraft ($w' < -w_T$) and near zero ($-w_T < w' < w_T$) components, where w' is the difference between the instantaneous vertical wind speed and w_o . The threshold velocity, $w_T = 0.5 \sigma_w$, was selected to maximize the signal-to-noise ratio of $(C_u - C_d)$. *Oncley et al.* [1993] discuss the choice of w_T in some detail and conclude that a value of around $0.6 \sigma_w$ is optimal.

Estimates of β and σ_w were calculated for each 27-min sampling period using wind and temperature data stored in digital format at 10 Hz. Coordinate transformations were performed on wind velocity data to set the mean vertical wind speed to zero. Estimates of β were calculated by assuming similarity between isoprene and sensible heat fluxes. Eddy covariance estimates of sensible heat flux, $\overline{w'T'}$, and the mean temperatures associated with updrafts and downdrafts, T_u and T_d , were used to estimate β by rearranging (2) and substituting $\overline{w'T'}$ for F , T_u for C_u and T_d for C_d .

Mixed layer. The tethered balloon profiling system consists of a commercial helium-filled tethered balloon and meteorological sounding system (AIR, Boulder, Colorado) and a custom made whole air sampling unit that attaches to any point on the tether line and pumps air into 15-L Teflon bags. Automatic timers were used to collect 30-min samples simultaneously at two to four heights between 50 and 800 m AGL. Whole air samples were analyzed for isoprene by the GC-FID method described in section 2.3. Isoprene fluxes were calculated using the mixed layer mass balance (MB) and mixed layer gradient (MLG) techniques.

The MB method assumptions and associated uncertainties are discussed by *Guenther et al.* [1996]. MB fluxes are calculated as

$$F = z_i C_m \tau^{-1} \quad (3)$$

where z_i is the mixed layer height (m AGL), τ is the estimated lifetime of isoprene (s), and C_m (milligrams carbon per cubic meter) is the mean mixed layer isoprene concentration. Estimates of z_i were obtained using airsondes (AIR, Boulder, Colorado) that measure temperature and humidity profiles up to heights of 5 km AGL. The mixed layer height was identified by an inversion layer that appears as a region of increasing potential temperature with height. To estimate the lifetime of isoprene, τ , we used the OH and ozone reaction rate coefficients reported by *Atkinson*, 1990], the measured ozone concentration, the OH diurnal variation described by *Lu and Khalil* [1991] and a maximum OH concentration of 4×10^6 molecules cm⁻³ [*Guenther et al.*, 1996]. We obtain C_m by fitting the observations to a specified vertical profile shape [*Guenther et al.*, 1996] and then computing the vertical average of this profile. Fluxes estimated by the MB technique are representative of an area about 14 km upwind of the measurement site (shown as the MB region in Plate 1).

Fluxes estimated by the MLG technique are dependent on z_i and the convective velocity scale, w_* . A major advantage of this technique is that it does not depend directly on estimates of OH concentrations. The MLG equations and assumptions are described in detail elsewhere [*K. Davis and D. Lenschow*, Scalar profiles and fluxes in the mixed layer, submitted to *Boundary Layer Meteorology*, 1996; *Guenther et al.*, 1996]. Fluxes estimated by the MLG technique are representative of an area about 3 km upwind of the measurement site (shown as the MLG region in Plate 1).

2.3. Isoprene Analysis

The GC-RGD and GC-FID systems deployed at the field site were intercalibrated using a compressed gas standard containing 71-ppbv isoprene referenced to a National Institute of Standards and Technology (NIST) propane standard on the GC-FID. Compound identification was accomplished by retention time comparison with known standards and by GC with mass spectrometer (MS) analysis of samples transported in stainless steel canisters to Boulder, Colorado. The isothermal GC-RGD system has a 2-mL sample loop, a stainless steel column (1.3m long \times 2mm ID) packed with Unibeads 3S, 60/80 mesh (Alltech Assoc., Deerfield, Illinois), and an RGD2 (Trace Analytical, Menlo Park, California) detector. This system does not require any preconcentration for isoprene mixing ratios above 1 ppbv and is described in detail elsewhere [*Greenberg et al.*, 1993].

The Hewlett-Packard 5890 GC-FID system was equipped with a 30-m DB-1 fused silica capillary column (J&W Scientific). A 100-500 mL whole air sample was preconcentrated on a cryogenically (liquid O₂) cooled stainless steel loop containing 60-80 mesh silanized glass beads. The concentrated samples were transferred to the GC column by immersing the loop in an 80°-90°C water bath. The GC oven was temperature programmed from -50°C to 80°C at 4°C min⁻¹.

2.4. Isoprene Emission Model

Isoprene emission rates, E ($\mu\text{g C g}^{-1} \text{ h}^{-1}$), for individual leaves or branches are modeled as

$$E = \epsilon \gamma \delta \quad (4)$$

where ϵ is an isoprene emission capacity ($\mu\text{g C g}^{-1} \text{h}^{-1}$) that represents the emission rate expected for a particular plant species at specified conditions (e.g., sun leaf during peak growing season, leaf temperature of 30°C and PAR of $1000 \mu\text{mol m}^{-2} \text{s}^{-1}$). The nondimensional emission activity factor, γ , accounts for variations in emissions due to changes in leaf temperature and PAR and is estimated using the equations of *Guenther et al.* [1993]. Leaf level estimates of γ can be estimated directly from leaf level PAR and leaf temperature. Branch level estimates are divided by a factor of 1.75 to account for decreases in PAR due to self shading [*Guenther et al.*, 1994]. A second nondimensional emission activity factor, δ , accounts for the longer-term variations in emissions due to season, phenology, growth environment, and other factors. All sun leaves and branches are assigned a value of $\delta = 1$ while shade leaves are assigned a value of $\delta = 0.8$ [*Harley et al.*, 1996a; *P. Harley et al.*, 1996b].

Model estimates of area-averaged isoprene fluxes ($\mu\text{g C m}^{-2} \text{h}^{-1}$) are calculated as

$$F = \epsilon \gamma \delta D \quad (5a)$$

where D is total foliar density ($\text{g dry weight m}^{-2}$) and ϵ , γ , and δ are all area-averaged estimates of corresponding leaf level parameters. The area-averaged ϵ represents the weighted average of all plant species within the area.

$$\epsilon = (\epsilon_{\text{OAK}} D_{\text{OAK}}) + (\epsilon_{\text{PINE}} D_{\text{PINE}}) + (\epsilon_{\text{MAPLE}} D_{\text{MAPLE}}) + \dots \quad (5b)$$

where D_{OAK} is the ratio of oak foliage to total foliage. Since oak trees are estimated to be responsible for over 95% of all isoprene emissions in each of the regions shown in Plate 1, we can simplify the following discussion by multiplying F by a factor A , equal to the fraction of total isoprene emissions contributed by oaks, and then neglecting isoprene emissions from vegetation other than oaks:

$$FA = (\epsilon_{\text{OAK}} D_{\text{OAK}}) \gamma \delta D \quad (6a)$$

We can compare the results from each measurement technique by inverting (6a) and solving for ϵ_{OAK} .

$$\epsilon_{\text{OAK}} = FA / [\gamma \delta D D_{\text{OAK}}] \quad (6b)$$

Total foliar density, D , and the fraction of oaks, D_{OAK} , for the SL, MB, and MLG regions were estimated using the techniques described in section 2.1. Canopy-averaged γ and δ were estimated by dividing the canopy into "sun" and "shade" leaf components and using the leaf level procedures described above. Estimates of PAR for sun leaves and for shade leaves were based on measured leaf area index (LAI) and above-canopy PAR and calculated sun angle using the sun-fleck radiative transfer model of *Norman* [1982]. Relative humidity, wind speed, and ambient temperature near sun and shade leaves were estimated from above-canopy relative humidity, wind speed, and ambient temperature using vertical profiles similar to those of *Lamb et al.* [1993]. Leaf temperatures for the shade and sun leaves were then calculated from estimates of total radiation, ambient temperature, wind speed, and relative humidity using a leaf energy balance model [*Lamb et al.*, 1993]. To convert between the LAI values used in the radiative transfer model and the foliar density estimates used in the emission model, we assume that shade leaves have a

specific leaf weight that is 70% [*Geron et al.*, 1994; *P. Harley et al.*, 1996b] of the value used for sun leaves.

3. Flux Measurement Results

Isoprene fluxes measured with each of the systems listed in Table 1 and described in section 2 are reported in this section. The results are compared and used to evaluate emission model procedures in section 4.

3.1. Leaf and Branch Fluxes

Isoprene fluxes from tree species of nine different genera were investigated with the BRS enclosure system. All of the sampled trees were growing within the MB region (Plate 1). Negligible isoprene emission rates were observed for six species: *Liriodendron tulipifera*, *Oxydendrum arboreum*, *Carya tomentosa*, *Sassafras albidum*, *Cornus florida*, and *Prunus serotina*. Significant isoprene emission rates were observed for species of *Quercus*, *Nyssa*, and *Liquidambar*. These results agree with the emission database compiled by *Guenther et al.* [1994]. An average emission rate of $1 \mu\text{g C g}^{-1} \text{h}^{-1}$ ($n=10$) determined for *Nyssa sylvatica* was representative of very low light levels (mean PAR= $85 \mu\text{mol m}^{-2} \text{s}^{-1}$) and a mean temperature of 24.5°C . Considerably higher mean isoprene emission rates were measured for *Liquidambar styraciflua* ($9.5 \mu\text{g g}^{-1} \text{h}^{-1}$, $n=14$), *Q. alba* ($14.1 \mu\text{g C g}^{-1} \text{h}^{-1}$, $n=16$), *Q. prinus* ($29.4 \mu\text{g C g}^{-1} \text{h}^{-1}$, $n=15$) and *Q. velutina* ($49.0 \mu\text{g C g}^{-1} \text{h}^{-1}$, $n=10$). The mean PAR for each set of measurements ranged from 180 to $462 \mu\text{mol m}^{-2} \text{s}^{-1}$, while mean leaf temperatures ranged from 24.2° to 30.0°C . The oak emission capacities listed in Table 2 range from 75 to $114 \mu\text{g C g}^{-1} \text{h}^{-1}$. These emission capacities are corrected for self shading and are representative of a leaf temperature of 30°C and PAR of $1000 \mu\text{mol m}^{-2} \text{s}^{-1}$.

The LEC, LNC, and BCS systems were used to measure emissions from a single mature *Q. alba* tree located adjacent to the walkup tower. The BCS system averaged a large number of leaves (15 to 30) with each measurement and was used to compare leaf and branch measurements. Individual leaf emission rates were estimated for a large number of leaves with the LNC system. The LEC system was used to investigate emission rate variations associated with changes in PAR and leaf temperature and to investigate leaf-to-leaf variation at constant PAR and temperature. Leaves near the top of the canopy typically had isoprene emission rates of less than $0.1 \mu\text{g C g}^{-1} \text{h}^{-1}$ before 700 local standard time (LST) and after 1700 LST with peak emission rates of over $150 \mu\text{g C g}^{-1} \text{h}^{-1}$ in early afternoon, associated with PAR fluxes over $1000 \mu\text{mol m}^{-2} \text{s}^{-1}$ and leaf temperatures over 33°C . Peak emissions for leaves lower in the canopy were as high as $100 \mu\text{g C g}^{-1} \text{h}^{-1}$ and occurred at times ranging from morning to late afternoon depending on their position relative to sunfleck gaps in the canopy.

3.2. Surface Layer Fluxes

Isoprene fluxes in the surface layer above the forest canopy were measured by relaxed eddy accumulation and a gradient profile method. The objectives of these surface layer flux measurements included (1) testing the REA system, (2) comparing REA and GPEC estimates of isoprene fluxes, and (3) evaluating the results of isoprene emission models with above-canopy flux measurements.

Table 2. Comparison of Isoprene Flux Measurement Techniques and Emission Model Variables

Measurement Technique	Cases	N	Measured Flux	Emission Model Variables				
				ϵ_{OAK}	γ	δ	D_{OAK}	D
<i>Leaf</i>								
LEC	Sunlit Leaves	8	99±2 ^a	99	1.0	1.0		
LEC	Shaded Leaves	8	89±2 ^a	111	1.0	0.8		
LNC	Sunlit Leaves	49	78±4 ^a	91	0.86	1.0		
LNC	Shaded Leaves	9	50±9 ^a	105	0.59	0.8		
<i>Branch</i>								
BCS	Sunlit Branch	7	54±5 ^a	102	0.53	1.0		
BCS	Shaded Branch	29	25±2 ^a	101	0.31	0.8		
BRS	<i>Q. alba</i>	16	28±1 ^a	75	0.46	0.8		
BRS	<i>Q. prinus</i>	15	27±4 ^a	110	0.31	0.8		
BRS	<i>Q. velutina</i>	10	21±2 ^a	114	0.23	0.8		
<i>Surface layer</i>								
REA	(PAR>250)	52	4.8±0.6 ^b	102	0.32	0.85	0.40	420
GPEC	(PAR>250)	27	4.0±0.7 ^b	86	0.34	0.85	0.40	420
<i>Mixed layer</i>								
MB	All cases	29	2.4±0.3 ^b	102	0.39	0.86	0.20	380
MB	Strong convection	8	2.8±0.7 ^b	122	0.41	0.86	0.20	380
MLG	Strong convection	8	5.0±1.7 ^b	148	0.41	0.86	0.24	400

Isoprene flux units include ^a $\mu\text{g C g}^{-1} \text{h}^{-1}$ and ^b $\text{mg C m}^{-2} \text{h}^{-1}$. N is the number of flux measurements. Emission model components are described by equations 5 and 6 and include oak (*Quercus*) emission rate capacity (ϵ_{OAK} , $\mu\text{g C g}^{-1} \text{h}^{-1}$), emission activity factors (γ and δ), total foliar density (D, $\text{g dry weight m}^{-2}$), and the oak fraction of total foliar density (D_{OAK}).

CO₂ and Water Vapor Fluxes. The accuracy of the CO₂ and water vapor fluxes estimated by direct eddy correlation with the open path IRGA (EC-O) has been established in previous studies [Baldocchi and Harley, 1995; Verma et al., 1986]. Fluxes estimated with the EC-O system are used here to evaluate fluxes estimated by direct eddy correlation with a closed path IRGA (EC-C) and by relaxed eddy accumulation. The corrections proposed by Webb et al. [1980] to account for density fluctuations were applied to the EC-O flux estimates but not to the EC-C measurements since heat transfer through the sampling tube should dampen temperature fluctuations. The EC-C and EC-O systems were colocated for over 50 half-hour sampling periods. CO₂ fluxes estimated with the two systems were within $\pm 5\%$ and were strongly correlated ($r^2 = 0.99$). The cospectra and power spectra calculated from the two analyzers agree for both CO₂ and water vapor.

Slightly different sampling periods were used for the REA (27 min) and EC-O (30 min) systems. Air passed through a relatively short length of tubing (3 m) prior to reaching the valve that directed the sample into the up or down reservoir. We assume that there is minimal dampening of temperature fluctuations and so have applied the Webb et al. [1980] density corrections. This may result in an overestimate of CO₂ fluxes for late morning and midday when sensible heat fluxes are highest. The REA and EC-O estimates of CO₂ fluxes shown in Figure 1 follow the expected diurnal pattern of low fluxes in early morning, maximum downward (negative) fluxes at midday, followed by decreasing fluxes into the evening. The mean REA CO₂ flux estimate ($-0.45 \pm 0.07 \text{ mg m}^{-2} \text{s}^{-1}$) is 13% greater than the mean flux ($-0.40 \pm 0.06 \text{ mg m}^{-2} \text{s}^{-1}$) calculated with the EC-O system. The mean REA flux is 43% greater if density corrections [Webb et al., 1980] are not applied. The scatterplot shown in Figure 2 indicates that there is only a moderate correlation ($r^2=0.45$) between the REA and EC-O flux estimates. The REA system slightly over-

estimates the lowest CO₂ fluxes and slightly underestimates the highest fluxes.

REA Isoprene Flux Estimates. Isoprene fluxes were estimated with the REA system for 59 sampling periods (~27 min). The three variables that determine isoprene fluxes calculated by the REA method, and the resulting isoprene flux, are shown for August 5 in Figure 3. Variations in ($C_u - C_d$) dominate the

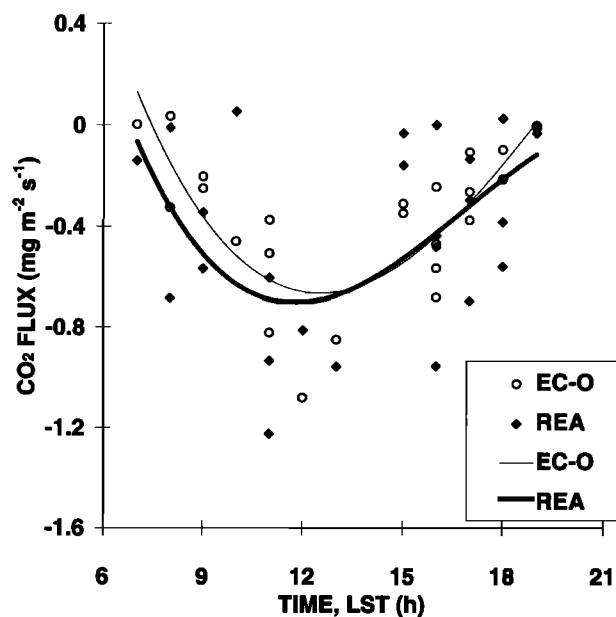


Figure 1. Diurnal variations in above-canopy CO₂ fluxes estimated with an eddy correlation (EC-O) system and a relaxed eddy accumulation (REA) system. A best fit third-order polynomial is shown as a dashed (EC-O) or solid (REA) line. Times are local standard time.

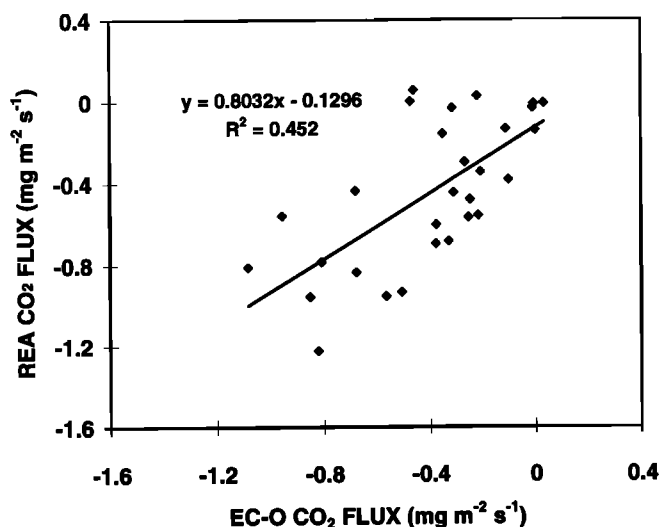


Figure 2. Comparison of above-canopy CO_2 fluxes estimated with an eddy correlation (EC-O) system and a relaxed eddy accumulation (REA) system.

resulting diurnal pattern of isoprene fluxes (Figure 3). The REA isoprene fluxes cover a period of 6 days (Julian date 213 to 218, Figure 4). The standard deviation of vertical wind speed (σ_w) ranged from $<0.3 \text{ m s}^{-1}$ (at night) to $>0.6 \text{ m s}^{-1}$ (midday). The observed estimates of $(C_u - C_d)$ increased from morning values of $\pm 0.5 \mu\text{g C m}^{-3}$, reaching $>15 \mu\text{g C m}^{-3}$ at midday and fell to $<-1 \mu\text{g C m}^{-3}$ in the evening. The calculated fluxes range from -1.4 to $15.8 \text{ mg C m}^{-2} \text{ h}^{-1}$, with a mean of $4.2 \pm 0.6 \text{ mg C m}^{-2} \text{ h}^{-1}$, and follow the expected pattern of increasing emissions with increasing PAR and temperature. PAR fluxes above the canopy were $<450 \mu\text{mol m}^{-2} \text{ s}^{-1}$ during 14 of the measurement periods. The mean flux of $0.05 \text{ mg C m}^{-2} \text{ h}^{-1}$ observed for these low-light conditions is dominated by deposition (downward) fluxes. Downward isoprene fluxes were estimated for 11 (19%) sampling periods. Isoprene deposition fluxes of -0.02 to -1.4 (mean $= -0.6$) $\text{mg C m}^{-2} \text{ h}^{-1}$ were estimated for these periods which typically occurred before 800 or after 1700 h LST. These results indicate that deposition fluxes may be significant but are much less than midday emission fluxes. When only upward isoprene fluxes are considered, the mean flux of $0.9 \text{ mg C m}^{-2} \text{ h}^{-1}$ for low light conditions (average PAR flux of $337 \mu\text{mol m}^{-2} \text{ s}^{-1}$ and ambient temperature of 23.7°C) is almost an order of magnitude lower than the mean flux of $5.9 \text{ mg C m}^{-2} \text{ h}^{-1}$ at high light conditions (average PAR of $1140 \mu\text{mol m}^{-2} \text{ s}^{-1}$ and ambient temperature of 25.1°C).

GPEC Isoprene Flux Estimates. Half-hour average isoprene fluxes were estimated during 30 sampling periods over seven days with the GPEC system described above. The GPEC system used water vapor gradients and direct eddy correlation flux measurements to estimate eddy diffusivities and should not be influenced by roughness sublayer effects. Observed isoprene gradients ranged from -0.17 to 0.73 (mean $= 0.26$) $\mu\text{g C m}^{-1}$ and were associated with eddy diffusivities of $4.0 \pm 0.6 \text{ m}^2 \text{ s}^{-1}$. The GPEC isoprene flux estimates (Julian date 208 to 214, Figure 4) range from $<-1 \text{ mg C m}^{-2} \text{ h}^{-1}$ to $>10 \text{ mg C m}^{-2} \text{ h}^{-1}$. The mean GPEC flux estimate for high-light ($>450 \mu\text{mol m}^{-2} \text{ s}^{-1}$) conditions is $4.8 \pm 0.8 \text{ mg C m}^{-2} \text{ h}^{-1}$. These fluxes represent a mean PAR of $850 \mu\text{mol m}^{-2} \text{ s}^{-1}$ and

ambient temperature of 26.1°C , which is similar to the conditions observed for the high-light sampling periods of the REA system. For high-light conditions, the mean isoprene flux estimated by the GPEC system is 20% lower than the mean flux estimated by REA.

Negative isoprene gradients (increasing isoprene concentration with height) greater than 0.05 mg C m^{-1} were observed during four of the 30 sampling periods. The negative gradients were all observed in the afternoon between 1500 and 1700 h LST. The downward fluxes ranged from -0.2 to $-2.0 \text{ mg C m}^{-2} \text{ h}^{-1}$ with an average deposition of $-1.2 \text{ mg C m}^{-2} \text{ h}^{-1}$.

3.3. Mixed Layer Fluxes

Isoprene mixing ratios in the atmospheric boundary layer above the Walker Branch field site range from less than 0.2 to greater than 5 ppbv isoprene. These data (Figure 5) represent samples collected at heights up to 800 m AGL during 29 half-hour sampling periods over a 2-week period. The mean mixed layer ($>160 \text{ m AGL}$) isoprene mixing ratio of 0.8 ppbv is 56% less than the mean mixing ratio of 1.8 ppbv for the surface layer ($<150 \text{ m AGL}$). Guenther et al. [1996] observed a similar mean isoprene mixing ratio (1.7 ppbv) in the surface layer

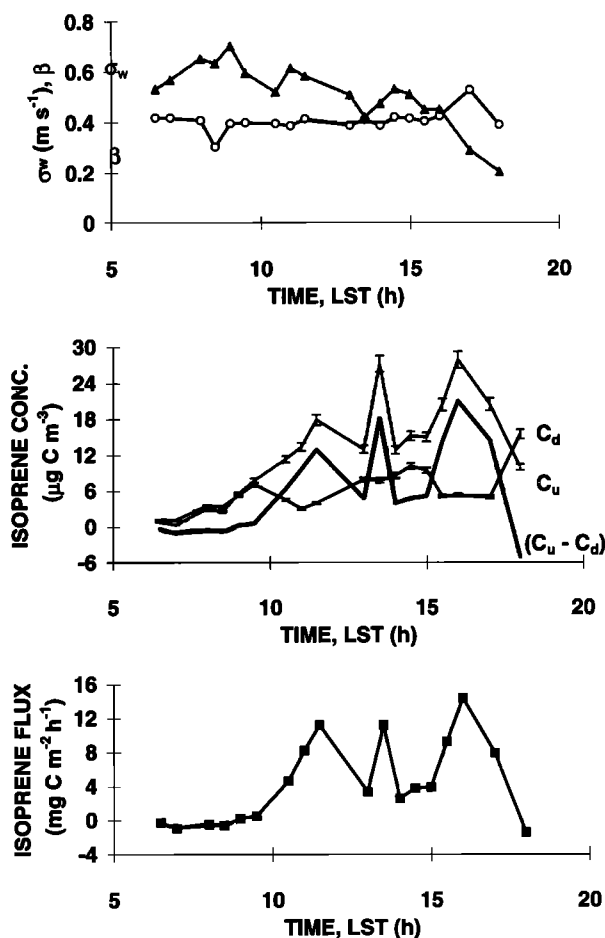


Figure 3. (bottom) Isoprene fluxes on August 5, 1992 estimated by relaxed eddy accumulation (REA) as the product of (top) the standard deviation of vertical wind speed (σ_w) and the empirical coefficient β , and (middle) the isoprene concentrations associated with updrafts (C_u) and downdrafts (C_d). Times are local standard time.

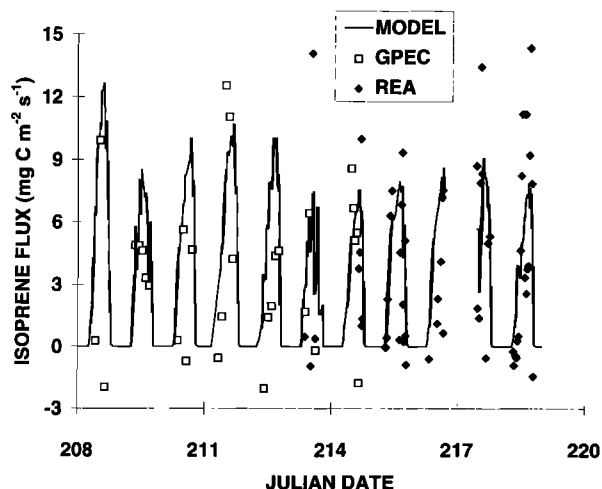


Figure 4. Above-canopy surface layer isoprene fluxes on Julian dates 208 to 219 (July 26 to August 5) estimated with the relaxed eddy accumulation (REA) and gradient profile with eddy correlation (GPEC) systems and predicted with equation 5 (MODEL).

above a mixed forest site in the state of Georgia, but a much higher (1.4 ppbv) mean mixing ratio in the mixed layer, equivalent to an 18% decrease. Analysis of paired (surface layer and mixed layer) samples at the Georgia field site showed a mean decrease of 38% between surface and mixed layers. These results demonstrate that there are considerable uncertainties associated with using surface layer measurements to predict isoprene mixing ratios in the mixed layer.

The diurnal patterns of the three variables required to estimate fluxes by the MB method and the resulting isoprene fluxes are shown in Figure 6. Estimates of the mixed layer cap-

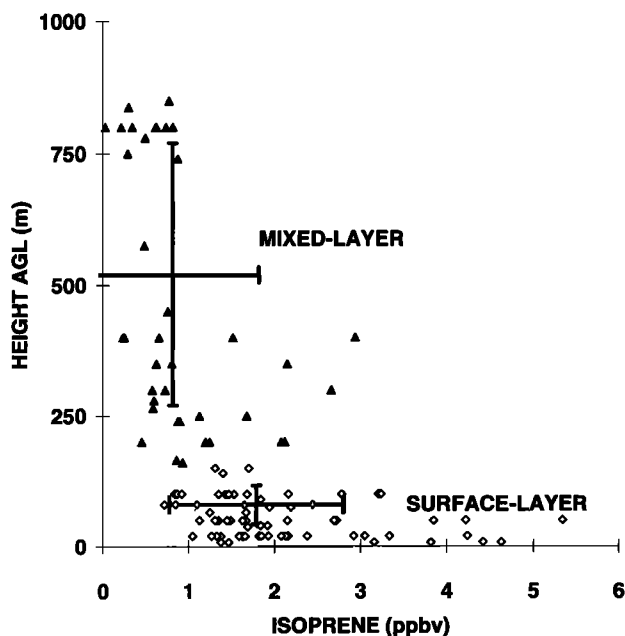


Figure 5. Thirty-minute average isoprene mixing ratios measured with the tethered balloon sampling system. The mean and standard deviations for altitude and mixing ratio are shown for mixed layer and surface layer samples.

ping inversion height vary from under 300 m AGL before 900 h LST to over 1200 m AGL after 1500 h LST. Estimates of the lifetime of isoprene (about 40 min) and the mean mixed layer isoprene mixing ratio (about 0.8 ppbv) were nearly constant between the hours of 900 and 1500 LST. The resulting isoprene flux estimates range from 0.5 to 7.6 mg C m⁻² h⁻¹, with a mean isoprene flux of 2.4 ± 0.3 mg C m⁻² h⁻¹. The mean PAR of 1150 $\mu\text{mol m}^{-2} \text{s}^{-1}$ and ambient temperature of 26.0°C for these 29 sampling periods are slightly higher than the mean PAR and temperature recorded during the REA and GPEC sampling periods for high light (PAR > 450 $\mu\text{mol m}^{-2} \text{s}^{-1}$). The MB flux source region (Plate 1) has a considerably lower density of isoprene emitting foliage than the SL region that is the source of the REA and GPEC fluxes. This is probably responsible for the 56% lower mean flux estimated with the MB method than for the REA system and 44% lower than the mean GPEC flux estimate.

Isoprene mixing ratio profiles were used to estimate fluxes using the mixed layer gradient technique described in section 2.2. Eight of the 29 sampling periods were suitable for calculating fluxes with the MLG method (i.e., significant surface heat flux and minimal cumulus cloud cover). Isoprene fluxes for these eight sampling periods were estimated to be 5.0 ± 1.7 mg C m⁻² h⁻¹. The observed profiles and fits are shown in Figure 7. The amount of isoprene emitting foliage in the MLG region shown in Plate 1 is about 25% higher than in the MB region. The mean MB flux estimate for the same eight sampling periods was 2.8 ± 0.7 mg C m⁻² h⁻¹ which is about 57% lower than the MLG flux estimates. These findings of lower MB and

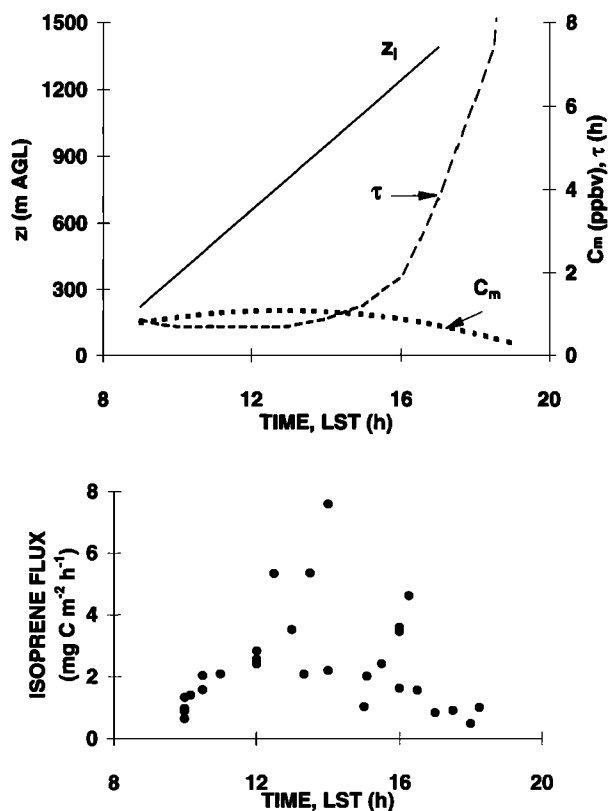


Figure 6. (bottom) Isoprene fluxes calculated with the mass balance (MB) technique as the product of mixed layer capping inversion height (z_i), isoprene lifetime (τ), and the mean mixed layer isoprene mixing ratio (C_m). Times are local standard time.

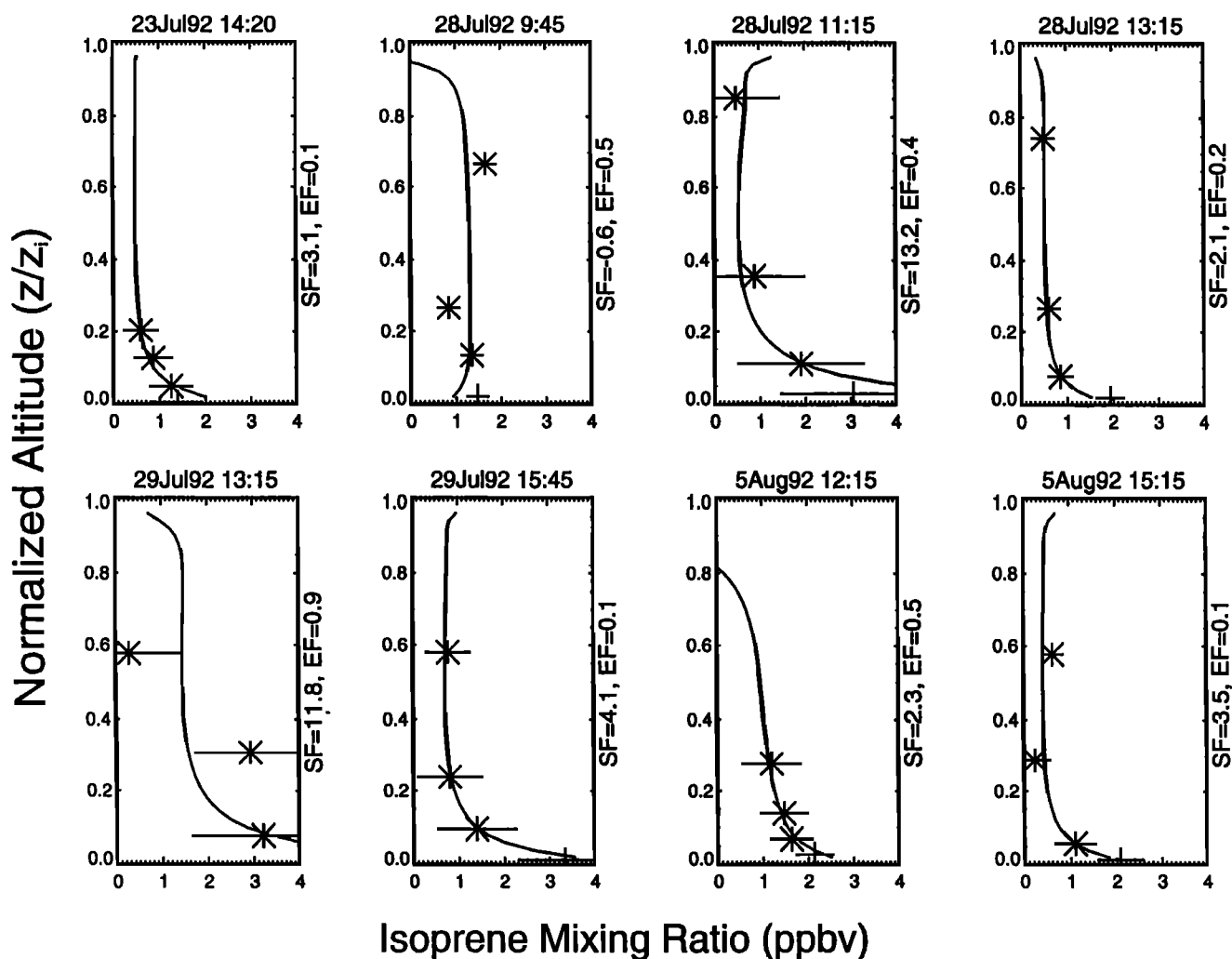


Figure 7. Isoprene profiles used to calculate fluxes using the MLG technique. The profile fit (solid line) is calculated from the MLG-derived fluxes and large eddy simulation (LES) generated gradient functions. Observed isoprene mixing ratios are marked with asterisks or crosses, where only asterisks were used to calculate fluxes. Horizontal bars through these points are theoretical estimates of error variance. Times are local standard time. SF and EF values to the right of each profile are the computed surface and entrainment fluxes, respectively, in units of $\text{mg C m}^{-2} \text{ h}^{-1}$.

higher MLG flux estimates are consistent with the discussion of Guenther *et al.* [1996] which predicts that the MB method should systematically underestimate fluxes, while the MLG technique may be prone to overestimates.

4. Emission Model Evaluation

The isoprene emission models described in section 2.4 require accurate estimates of oak emission capacity (ϵ_{OAK}), emission activity factors (γ and δ), total foliar density (D) and the fraction of foliage that is oak leaves (D_{OAK}). Table 2 includes estimates of each of these variables and the actual fluxes estimated with each of the eight techniques (section 2, Table 1).

4.1. Foliar Density, D , and Fraction of Oak Foliage, D_{OAK}

Oak foliar densities range from 0 to 282 g m^{-2} within the 31 circular 30-m diameter sample plots. These plots have an aver-

age tree foliar density of 366 g m^{-2} and a leaf area index of $4.9 \text{ m}^2 \text{ m}^{-2}$ dominated by *Quercus* (95 g m^{-2}) and *Pinus* (88 g m^{-2}). The remaining forest is dominated by deciduous trees, primarily species of *Cornus* (26 g m^{-2}), *Acer* (22 g m^{-2}), *Liriodendron* (22 g m^{-2}), and *Oxydendrum* (15 g m^{-2}).

The 12 sampling plots within the SL region are located at distances ranging from 15 to 610 m from the tower. Oak foliar densities were highly variable along the transect with values ranging from 258 g m^{-2} at the plot centered at 15 m from the tower to less than 2 g m^{-2} in the sampling plots at 135 m from the tower and between 300 and 500 m from the tower. Lamb *et al.* [1996] report results of three methods of estimating oak foliar density along this transect: an arithmetic average of 110 g m^{-2} , a distance weighted average of 220 g m^{-2} and a footprint weighted average of 203 g m^{-2} . The footprint weighted average is assumed to be the best estimate.

The 30-m resolution Landsat TM land cover (TMLC) database indicates that 98% of the SL region, 82% of the MLG landscape region and 70% of the MB landscape region are

covered by one of six forest land cover types. The TMLC estimates of total foliar density shown in Table 2 range from 420 g m⁻² in the SL region to 400 g m⁻² in the MLG region and 380 g m⁻² in the MB region. The total foliar density predicted by the BEIS2 model for the three counties surrounding the field site is about 40% less than the TMLC estimate for the MB region. Table 2 shows that the TMLC estimates of D_{OAK} include 0.20 in the MB region, 0.24 in the MLG region and 0.40 in the SL region. The BEIS2 estimates of D_{OAK} for the three-county area (0.42) is a factor of 2 higher than the TMLC estimate for the MB region.

The TMLC estimate of oak foliar density in the SL region is 168 g m⁻². The various estimates of *Lamb et al.* [1996] are within about $\pm 50\%$ of this value. Considerably lower oak foliar densities are estimated by the TMLC database for the MLG (96 g m⁻²) and MB (76 g m⁻²) regions. The TMLC estimate for the MB region is within about 25% of the BEIS2 model estimate for the three-county area. These results indicate that estimates of oak foliar densities are associated with uncertainties of $\pm 50\%$ or less.

4.2. Emission Activity Factors, γ and δ

The enclosure measurement systems were used to investigate emission activity factors. The results summarized in this section are described in detail by P. Harley et al., (1996b). The LNC and LEC systems both estimate that shade leaf emissions are about 10% less than sun leaf emissions. This is equivalent to assigning shade leaves a value of $\delta = 0.9$. Measurements from the BCS system result in a value of $\delta = 0.79$ for shaded branches. The LEC, LNC, and BCS enclosure systems were also used to evaluate the light and temperature dependent algorithms developed by *Guenther et al.* [1993] to estimate γ . The results demonstrate that these algorithms can simulate the observed isoprene emission rate variations in the top of a mature tree canopy to within $\pm 15\%$ for midday conditions.

A tree branch with a PAR flux of 1000 $\mu\text{mol m}^{-2} \text{s}^{-1}$ at the top of the branch has PAR fluxes on individual leaves that range from less than 100 to 1000 $\mu\text{mol m}^{-2} \text{s}^{-1}$ due to leaf angle orientation and shading by upper leaves. In addition, the temperature of various leaves on a branch may differ by several degrees. *Guenther et al.* [1994] recognized that the emission activity factor applied to a branch must be adjusted to account for these effects. They noted that field comparisons of the ratio between leaf and branch level emission rates range from 1.46 to 2.03 [*Guenther et al.*, 1996] and recommended that γ be divided by a factor of 1.75 for branch measurements. We evaluated this ratio by measuring isoprene emission rates for whole branches and individual leaves within the canopy of a mature oak (*Q. alba*) tree with the BCS and LNC systems. The ratio of leaf-to-branch emission rates was 1.92 near the top of the canopy and decreased to 1.69 in the middle of the canopy. The radiative transfer model and emission algorithms described in section 2.4 predict that this ratio will vary between 1.3 and 1.9 depending on branch LAI, mean leaf orientation angle, and solar elevation. This ratio increases with decreasing mean leaf angle, increasing LAI and decreasing solar elevation. These results support the *Guenther et al.* [1994] recommendation to estimate γ based on above branch PAR and temperature and then divide by 1.75 to calculate a branch average γ . An overall uncertainty of about $\pm 30\%$ is associated with estimates of γ for branch enclosure measurements.

Uncertainties in estimating γ for an entire forest canopy are greater than those associated with branch measurements. *Lamb et al.* [1996] evaluated the canopy average estimates of γ predicted by five different canopy environment models for the REA and GPEC estimates. The complexity of these canopy environment models range from treating the canopy as a single leaf to a detailed numerical model that accounts for leaf-sun geometry, leaf energy balance, photosynthesis, transpiration, respiration, and gas transport within the canopy. The results indicate that the various models predict fluxes that are within approximately $\pm 20\%$. Additional uncertainties in the leaf level relationships (about $\pm 15\%$) and in estimating ambient temperature and above-canopy PAR (about $\pm 25\%$) result in an overall uncertainty of about $\pm 35\%$ for γ .

The diurnal patterns of predicted and observed fluxes for the entire study period (Figure 4) show positive fluxes between 700 and 1800 LST with a maximum occurring in early afternoon. The observed diurnal patterns are consistent with emission model predictions.

4.3. Emission Capacity, ϵ

Emission capacities for individual leaves or for an entire branch are calculated from (6) using the measured emission rate and an estimate of γ calculated from the algorithms described by *Guenther et al.* [1993]. Measurements of individual leaves at conditions where $\gamma = 1$ result in estimates of ϵ that have relatively low uncertainties ($\pm 10\%$). Uncertainties in ϵ are considerably higher when γ must be estimated from leaf temperature and PAR conditions that deviate substantially from standard conditions. Uncertainties in extrapolating ϵ obtained for a few leaves to all leaves in a forest belonging to a particular plant genus are often about $\pm 50\%$ [*Guenther et al.*, 1994]. Estimating emission capacities from area-averaged flux measurements have uncertainties associated with the flux measurements, the canopy environment model estimates of γ , and the requirement of foliar density estimates. Each of these three variables has an uncertainty of about $\pm 35\%$ resulting in an overall uncertainty of about $\pm 60\%$.

The BRS enclosure system estimates of isoprene emission capacities are $16 \pm 3 \mu\text{g C g}^{-1} \text{h}^{-1}$ ($n=10$) for *Nyssa sylvatica* and $64 \pm 7 \mu\text{g C g}^{-1} \text{h}^{-1}$ ($n=14$) for *Liquidambar styraciflua*. These results agree with published emission capacities [*Harley et al.*, 1996a; *Guenther et al.*, 1994] which include $70 \pm 35 \mu\text{g C g}^{-1} \text{h}^{-1}$ for *Liquidambar* species and $12 \pm 6 \mu\text{g C g}^{-1} \text{h}^{-1}$ for *Nyssa* species. Estimates of ϵ for the three oak species measured with the BRS system range from $75 \mu\text{g C g}^{-1} \text{h}^{-1}$ for *Q. alba* to $114 \mu\text{g C g}^{-1} \text{h}^{-1}$ for *Q. velutina*. Emission capacities estimated with the LEC, LNC, and BCS systems for a single *Q. alba* tree next to the walkup tower range from 91 to 111 $\mu\text{g C g}^{-1} \text{h}^{-1}$. The lowest uncertainty is associated with the isoprene emission capacity of $99 \mu\text{g C g}^{-1} \text{h}^{-1}$ estimated from measurements on sun leaves with a leaf temperature of 30°C and PAR of $1000 \mu\text{mol m}^{-2} \text{s}^{-1}$. Eight of the nine leaf and branch estimates of ϵ listed in Table 2 fall within the relatively narrow range of $100 \pm 11 \mu\text{g C g}^{-1} \text{h}^{-1}$.

Estimates of area-averaged oak emission capacities were estimated from above-canopy surface layer and mixed layer measurements and (6). The isoprene emission capacities estimated for oaks in the SL flux region include $86 \mu\text{g C g}^{-1} \text{h}^{-1}$ with the GPEC system and $102 \mu\text{g C g}^{-1} \text{h}^{-1}$ with the REA system. The MLG estimate of $148 \mu\text{g C g}^{-1} \text{h}^{-1}$ is the highest oak emission capacity listed in Table 2. The MB estimate for the same eight sampling periods used for the MLG estimates is

122 $\mu\text{g C g}^{-1} \text{ h}^{-1}$ and is about 20% higher than the mean emission capacity calculated for all 29 sampling periods. The surface layer estimates of oak isoprene ϵ ($94 \pm 8 \mu\text{g C g}^{-1} \text{ h}^{-1}$) are about 25% less than the mixed layer estimates of oak isoprene ϵ ($124 \pm 22 \mu\text{g C g}^{-1} \text{ h}^{-1}$).

The mean oak isoprene emission capacities for each measurement scale shown in Table 2 include 102 $\mu\text{g C g}^{-1} \text{ h}^{-1}$ for leaf enclosure measurements, 100 $\mu\text{g C g}^{-1} \text{ h}^{-1}$ for branch enclosure measurements, 94 $\mu\text{g C g}^{-1} \text{ h}^{-1}$ for above-canopy surface layer measurements, and 124 $\mu\text{g C g}^{-1} \text{ h}^{-1}$ for above-canopy mixed layer measurements. These results demonstrate that the emission model techniques, which enable us to estimate the oak isoprene emission capacity associated with each measurement, produce results within about $\pm 25\%$ which is within the uncertainties associated with these flux measurements. Significant deposition losses within the forest canopy would result in lower emission capacities estimated by the above-canopy flux measurement techniques. While one of the surface layer techniques (GPEC) had a somewhat lower estimated ϵ , the other techniques (REA, MB, MLG) resulted in oak isoprene emission capacities that were about equal to or higher than the emission capacities estimated from enclosure techniques. This result suggests that although it is likely that isoprene deposition losses occur, as indicated by the morning and evening surface layer flux measurements, they are a relatively minor component of the net flux. Thirteen of the fourteen emission capacities estimated in Table 2 are within $\pm 25\%$ of 100 $\mu\text{g C g}^{-1} \text{ h}^{-1}$ and the emission capacity estimated using the mixed layer gradient technique (148 $\mu\text{g C g}^{-1} \text{ h}^{-1}$) is even greater. These results demonstrate that the isoprene emission capacity for oak trees, in at least this region, is higher than the value used in existing models (70 $\mu\text{g C g}^{-1} \text{ h}^{-1}$ for BEIS2, 14.7 $\mu\text{g C g}^{-1} \text{ h}^{-1}$ for BEIS).

5. Summary

Eight flux measurement techniques were used to estimate isoprene fluxes from a temperate forest. Fluxes from individual leaves and branches were measured with enclosure systems, above-canopy fluxes were measured from a tower by relaxed eddy accumulation and surface layer gradients, and fluxes from landscapes covering an area of up to a few hundred square kilometers were estimated using a tethered balloon sampling system. Each measurement system provided specific advantages for investigating different aspects of biogenic emission models. The results from all measurement techniques demonstrate that existing emission models underestimate the isoprene emission capacity for oaks in this region and a value of 100 $\mu\text{g C g}^{-1} \text{ h}^{-1}$ is recommended. The results also demonstrate that reasonable estimates of isoprene fluxes and boundary layer isoprene mixing ratios can be predicted with existing models if accurate data (e.g., emission capacities and land characteristics data) are available for initializing the models. It is clear that considerable uncertainties exist in field flux measurements and in each of the main components of emission models. Research directed at narrowing these uncertainties and acquiring data for initializing models in other regions remains a priority for biogenic emission studies.

Acknowledgments. This research was partially supported by the Environmental Protection Agency, Research Triangle Park, North Carolina, under Interagency Agreement Grant No. DW49934973-01-0,

and by the Southern Oxidants Study (SOS) under Assistance Agreement No. CR817766 to North Carolina State University. The authors gratefully acknowledge Rick Lowe and Brett Taylor for assistance with field measurements and data analysis and Mike Huston of the Oak Ridge National Laboratory for assistance in characterizing the ecology of this region. We thank Detlev Helmig and Chris Cantrell of NCAR and two anonymous reviewers for helpful comments on this manuscript. The National Center for Atmospheric Research is sponsored by the National Science Foundation.

References

- Atkinson, R., Gas-phase tropospheric chemistry of organic compounds: A review, *Atmos. Environ.*, **24A**, 1-41, 1990.
- Baldocchi, D., A. Guenther, P. Harley, L. Klinger, P. Zimmerman, B. Lamb, and H. Westberg, The fluxes and air chemistry of isoprene above a deciduous hardwood forest, *Philos. Trans. R. Soc. Lond.*, **350**, 279-296, 1995.
- Businger, J., and S. Oncley, Flux measurement with conditional sampling, *J. Atmos. Oceanic Technol.*, **7** (2), 349-352, 1990.
- Geron, C., A. Guenther, and T. Pierce, An improved model for estimating emissions of volatile organic compounds from forests in the eastern United States, *J. Geophys. Res.*, **99**, 12,773-12,792, 1994.
- Geron, C., T. Pierce, and A. Guenther, Reassessment of biogenic volatile organic compound emissions in the Atlanta area, *Atmos. Environ.*, **29**, 1569-1578, 1995.
- Greenberg, J., P. Zimmerman, B. Taylor, G. Silver, and R. Fall, Subparts per billion detection of isoprene using a reduction gas detector with a portable gas chromatograph, *Atmos. Environ.*, **27**, 2689-2692, 1993.
- Guenther, A., Seasonal and spatial variations in natural volatile organic compound emissions, *Ecol. Appl.*, in press, 1996.
- Guenther, A., P. Zimmerman, P. Harley, R. Monson, and R. Fall, Isoprene and monoterpene emission rate variability: Model evaluation and sensitivity analysis, *J. Geophys. Res.*, **98**, 12,609-12,617, 1993.
- Guenther, A., P. Zimmerman, and M. Wildermuth, Natural volatile organic compound emission rate estimates for U.S. woodland landscapes, *Atmos. Environ.*, **28**, 1197-1210, 1994.
- Guenther, A., P. Zimmerman, L. Klinger, J. Greenberg, C. Ennis, K. Davis, H. Westberg, and E. Allwine, Estimates of regional natural volatile organic compound fluxes from enclosure and ambient measurements, *J. Geophys. Res.*, **101**, 1345, 1996.
- Harley, P., A. Guenther, and P. Zimmerman, Effects of light, temperature and canopy position on net photosynthesis and isoprene emission from leaves of sweetgum (*Liquidambar styraciflua* L.), *Tree Phys.*, **16**, 25-32, 1996a.
- Johnson, D., and R. van Hook, *Analysis of Biogeochemical Cycling Processes in Walker Branch Watershed*, pp. 401, Springer-Verlag, New York, 1989.
- Lamb, B., et al., Evaluation of forest canopy models for estimating isoprene emissions, *J. Geophys. Res.*, in press, 1996.
- Lamb, B., D. Gay, H. Westberg, and T. Pierce, A biogenic hydrocarbon emission inventory for the U.S. using a simple forest canopy model, *Atmos. Environ.*, **27**, 1673-1690, 1993.
- Lamb, B., H. Westberg, and G. Allwine, Biogenic hydrocarbon emissions from deciduous and coniferous trees in the United States, *J. Geophys. Res.*, **90**, 2380-2390, 1985.
- Lamb, B., H. Westberg, and G. Allwine, Isoprene emission fluxes determined by an atmospheric tracer technique, *Atmos. Environ.*, **20**, 1-8, 1986.
- Lu, Y., and M. Khalil, Tropospheric OH: Model calculations of spatial, temporal, and secular variations, *Chemosphere*, **23**, 397-444, 1991.
- Norman, J., Simulation of microclimates, in *Biometeorology in Integrated Pest Management*, Academic, San Diego, Calif., 1982.
- Oncley, S., A. Delany, T. Horst, and P. Tans, Verification of flux measurement using relaxed eddy accumulation, *Atmos. Environ.*, **27A**, 2417-2426, 1993.
- Pierce, T., and P. Waldruff, PC-BEIS: A personal computer version of the biogenic emissions inventory system, *J. Air and Waste Manage. Assoc.*, **41**, 937-941, 1991.
- Verma, S., D. Baldocchi, E. Anderson, D. Matt, and R. Clement, Eddy fluxes of CO_2 , water vapor and sensible heat over a deciduous forest, *Boundary Layer Meteorol.*, **36**, 71-91, 1986.

Webb, E., A. Pearm, and R. Leuning, Correction of flux measurements for density effects due to heat and water vapor transfer, *Q. J. R. Meteorol. Soc.*, 106, 85-100, 1980.

A. Guenther, W. Baugh, K. Davis, G. Hampton,¹ P. Harley, L. Klinger, L. Vierling, and P. Zimmerman, National Center for Atmospheric Research, P.O. Box 3000, Boulder, CO 80307. (e-mail: guenther@acd.ucar.edu)

G. Allwine, S. Dilts, B. Lamb, and H. Westberg, Department of Civil

and Environmental Engineering, Washington State University, Pullman, WA 99164.

D. Baldocchi, Atmospheric Turbulence and Diffusion Division, NOAA, Oak Ridge, TN 37830.

C. Geron, and T. Pierce, Office of Research and Development, U.S. Environmental Protection Agency, Research Triangle Park, NC 27711.

(Received October 16, 1995; revised January 29, 1996;
accepted February 27, 1996.)